
DIFFERENTIABLE SHORT-TIME FOURIER TRANSFORM WITH RESPECT TO THE HOP LENGTH

ACCEPTED FOR IEEE SSP WORKSHOP 2023

Maxime Leiber^{*†}, Yosra Marnissi[†], Axel Barrau[‡], Mohammed El Badaoui^{†§}

^{*} INRIA, DI/ENS, PSL Research University
[†] Safran Tech, Digital Sciences & Technologies
[‡] Offroad
[§] Univ Lyon, UJM-St-Etienne, LASPI

ABSTRACT

In this paper, we propose a differentiable version of the short-time Fourier transform (STFT) that allows for gradient-based optimization of the hop length or the frame temporal position by making these parameters continuous. Our approach provides improved control over the temporal positioning of frames, as the continuous nature of the hop length allows for a more finely-tuned optimization. Furthermore, our contribution enables the use of optimization methods such as gradient descent, which are more computationally efficient than conventional discrete optimization methods. Our differentiable STFT can also be easily integrated into existing algorithms and neural networks. We present a simulated illustration to demonstrate the efficacy of our approach and to garner interest from the research community.

Keywords time-frequency representation · short-time Fourier transform · spectrogram · differentiable · adaptive · window length · hop length · gradient descent

1 Introduction

The short-time Fourier transform (STFT) is a frequently used tool for analyzing non-stationary digital signals in various fields including audio Stafford et al. [1998], medicine Huang et al. [2019], and vibration analysis Leclère et al. [2016]. Spectrograms, which are obtained from the STFT magnitude, are essential for visualizing, understanding, and processing non-stationary signals in time-frequency representation.

The STFT parameters, including tapering function, window length, and hop length, are critical and dependent on the application and signal characteristics. The tapering function balances frequency resolution and spectral leakage, with a narrower main lobe providing better frequency resolution at the expense of increased spectral leakage, and a wider main lobe reducing spectral leakage but decreasing frequency resolution. The Hann or Hamming window is a common starting point, but the best choice depends on the application's specific requirements. Actually, most studies on STFT parameters have focused on the choice of the window length, as it determines the time-frequency resolution trade-off. A shorter window length provides better time resolution but poor frequency resolution. Conversely, a longer window length provides better frequency resolution but poor time resolution. To provide more precise control over temporal and frequency resolution based on the local characteristics of the input signal, researchers have proposed using variable-length windows. These methods are known as S transform Stockwell et al. [1996], Sejdić et al. [2007], Moukadem et al. [2015] and adaptive STFTs Czerwinski and Jones [1997], Kwok and Jones [2000], Zhong and Huang [2010], Pei and Huang [2012], Zhu et al. [2015]. Often, the optimal window lengths in the 2D plane are chosen to favor a particular criterion of sparsity Zhao et al. [2021], Jablonski and Dziedziech [2022], Pei and Huang [2012], Meignen et al. [2020]. Since these parameters are discrete, finding the optimal tuning is usually done using grid search or trial-and-error, which can be time-consuming. Differentiable versions of the STFT have been recently proposed Zhao

et al. [2021], Leiber et al. [2022a,b, 2023] making the window length a continuous parameter that can be optimized by gradient descent.

The third parameter in STFT, the hop length, controls the trade-off between temporal resolution and computational cost. The smaller the hop length is, the higher the temporal resolution is, allowing for more detailed changes in frequency content over time. Conversely, a larger hop length provides lower temporal resolution, which may be sufficient in applications such as music classification Choi et al. [2017] and sound event detection Parascandolo et al. [2016] where the focus is on identifying the presence of certain sound events rather than their exact temporal location. Additionally, in machine learning applications, the hop length choice can significantly impact model performance as a shorter hop length provides more detailed information about data but increases computational complexity. Note that, accurately identifying and localizing transient events is critical in many applications, such as bird call classification Acevedo et al. [2009], Koh et al. [2019] and vibration health monitoring tasks like shock characterization and angular position detection of harmonic sources Sadler et al. [1998], Chandra and Sekhar [2016]. Capturing the fine temporal structure of these events provides valuable insights and enables reliable analysis and diagnosis. However, accurate localization of these events can be challenging if the analysis window is not aligned with the beginning of the target components, leading to energy leakage in the spectrogram. Therefore, selecting the appropriate hop length is critical to capture the temporal dynamics of the signal, such as the attack and decay of the target components.

In summary, the optimal hop length value in spectrograms depends on the specific application and input signal characteristics. To the best of our knowledge, there has not been sufficient research on tuning or adapting the hop length to signal characteristics, as most applications use a fixed hop length. These fixed hop lengths are often set to default values in commonly used signal processing libraries or selected empirically by trial-and-error.

Our main contribution in this paper is the development of a differentiable version of the STFT, which allows for the easy optimization of the hop length (or frame index) per-frame using gradient descent. This is achieved by modifying the definition of the STFT operator to make the hop length a continuous parameter, with respect to which the STFT values can be differentiated. We utilize the continuity of the tapering function to differentiate with respect to the frame temporal position. The STFT operation is mathematically differentiable, and we provide the necessary calculations and formulas for propagation and backpropagation.

This paper is organized as follows: in Section 2, we provide definitions and notations for the STFT and the differentiable STFT. In Section 3, we introduce our modified differentiable STFT with respect to the hop length. In Section 4, we demonstrate the effectiveness of our approach with a simulated illustration. Finally in Section 5, we conclude with final remarks.

2 Background

2.1 Short-Time Fourier Transform

Throughout this paper, we refer to the short-time Fourier transform (STFT) as the operation that takes a one-dimensional signal $s[t]$ as input and returns a one-dimensional matrix $\mathcal{S}[i, \xi]$. Each column $\mathcal{S}[i, :]$ of the STFT is the discrete Fourier transform (DFT) of a slice of length L of the signal s , starting from an index b_i and ending at an index $b_i + L - 1$, multiplied by a tapering function ω_L of length L . The STFT can be mathematically written as:

$$\mathcal{S}[i, \xi] = \sum_{k=0}^{L-1} \omega_L[k] s[b_i + k] e^{-\frac{2j\pi k\xi}{L}} \quad (1)$$

The starting indices b_i of the time intervals on which spectra are computed are usually equally spaced, so we only need to set the first index b_0 and the spacing Δb between b_i and b_{i+1} . There are several choices of tapering function ω_L that can be used, such as the Gaussian and Hann windows.

2.2 Differentiable Short-Time Fourier Transform

Differentiable short-time Fourier transform (DSTFT) has been proposed in previous works Leiber et al. [2022a,b, 2023]. It modifies the definition of the STFT operator by making the window length a continuous parameter, enabling spectrogram values to be easily differentiated with respect to this parameter with gradient descent. This differentiable STFT can be readily integrated into any neural networks involving spectrograms, where the STFT can be made into a layer whose weights are the window lengths of the STFT, or can be optimized on-the-fly based on a criterion. The idea behind DSTFT is to separate the window length L into an *integer numerical window support* N and a *continuous time resolution* θ . Moreover, it is possible to define a continuous window length for each bin of the STFT, which provides a temporal resolution $\theta_{i,\xi}$ for each frame i and frequency ξ :

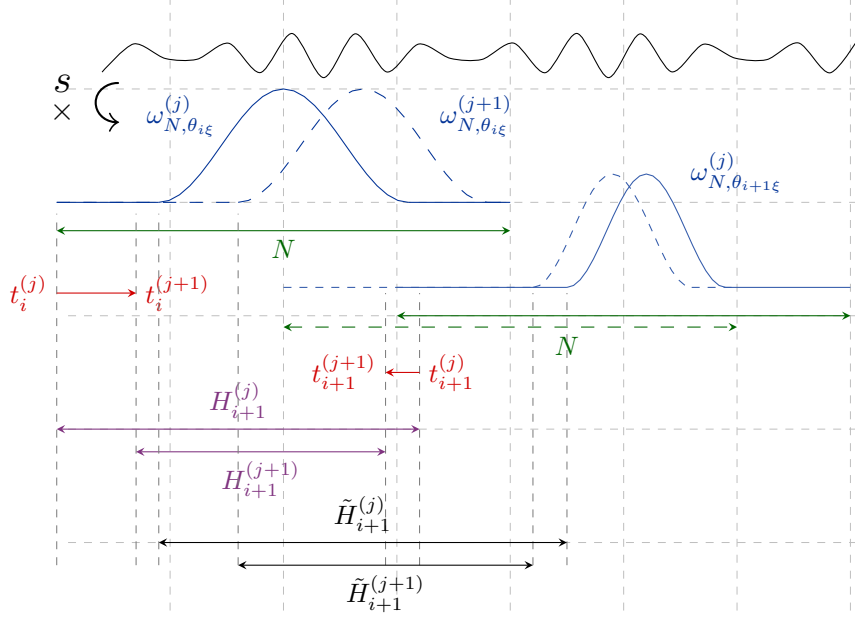


Figure 1: Differentiable STFT: The position of the tapering windows can smoothly shift along the time axis, while the window support starts at the integer part of the temporal position of the tapering windows. The exponent j denotes the iteration in the gradient descent optimizer.

$$\mathcal{S}[i, \xi] = \sum_{k=-\infty}^{+\infty} \omega_{N, \theta_{i\xi}}[k] s[t_i + k] e^{-\frac{2j\pi k\xi}{N}}, \quad (2)$$

where $\omega_{N, \theta_{i\xi}}$ is a tapering function defined on $[0, N - 1]$ (is zeros outside this interval) but taking non-zero (or non-negligible) values in the interval $\left[\frac{N-1-\theta_{i\xi}}{2}, \frac{N-1+\theta_{i\xi}}{2}\right]$.

3 Proposed method

In the same spirit as the differentiable STFT with respect to the window length, this section proposes a differentiable version of the STFT with respect to the hop length, allowing for optimization with gradient descent either locally on-the-fly (online) by minimizing an adaptive criteria for each signal, or globally (offline) by minimizing an overall performance measure of a given task over a dataset.

In the following, we assume that, the tapering functions $\omega_{N, \theta_{i\xi}}$ are continuous and differentiable, with continuous derivatives with respect to time t and window length θ . Examples of such functions are the Hann (Eq. 3) and the Gaussian (Eq. 4) functions, which are defined in the support $[0, N - 1]$ and have been presented in previous works on the DSTFT Leiber et al. [2022a,b, 2023], Zhao et al. [2021]:

$$\omega_{N, \theta}[k] = \frac{1}{2} - \frac{1}{2} \cos\left(\frac{2\pi k}{\theta}\right) \quad (3)$$

$$\omega_{N, \theta}[k] = \exp\left(-\frac{k^2}{2\left(\frac{\theta}{6}\right)^2}\right) \quad (4)$$

The STFT can be differentiated with respect to the hop length H_i by equivalently differentiating the STFT spectrum $\mathcal{S}[i, \xi]$ with respect to the temporal position t_i , where the hop length is the difference between two consecutive frames i.e $H_i = t_i - t_{i-1}$, $H_1 = t_1$. This is possible because the tapering function $\omega_{N, \theta_{i\xi}}$ is continuous and differentiable with respect to the temporal position t_i . However, there is one constraint: the analysis window must start on integer

values since the signal is discrete. To overcome this constraint, the window is started at $\lfloor t_i \rfloor$ as displayed in Fig. 1, and the effect of the integer part is compensated by a small shift $\{t_i\} = t_i - \lfloor t_i \rfloor$ in the argument of $\omega_{N,\theta_{i,\xi}}$ and a factor $e^{2j\pi\{t_i\}\xi/N}$. This makes this modified version of the STFT differentiable with respect to the frame index t_i (and equivalently the hop length H_i) and the window length $\theta_{i,\xi}$:

$$\mathcal{S}[i, \xi] = \sum_{k=-\infty}^{+\infty} \omega_{N,\theta_{i,\xi}}[k - \{t_i\}]s[\lfloor t_i \rfloor + k]e^{-\frac{2j\pi(k - \{t_i\})\xi}{N}} \quad (5)$$

The rest of this section will be devoted to the justification of the formula presented in Eq. (5) by showing that it is continuous and differentiable with respect to t_i .

Proposition 3.1. *The STFT defined by Eq. (5) is everywhere continuous with respect to the frame index t_i .*

Proof. The integer and fractional part functions are continuous everywhere except at integers. Therefore, Eq. (5) is continuous everywhere except possibly when t_i is an integer value $p \in \mathbb{N}$. We will prove that it is also continuous in this case by looking at its left and right limits, i.e. for $t_i = p \pm \epsilon$ as $\epsilon \rightarrow 0$.

For $t_i = p - \epsilon$, we have $\lfloor t_i \rfloor = p - 1$ and $\{t_i\} = 1 - \epsilon$, which implies:

$$\begin{aligned} \mathcal{S}[i, \xi] &= \sum_{k=-\infty}^{+\infty} \omega_{N,\theta_{i,\xi}}[k - 1 + \epsilon]s[p - 1 + k]e^{-\frac{2j\pi(k - 1 + \epsilon)\xi}{N}} \\ &= \sum_{k=-\infty}^{+\infty} \omega_{N,\theta_{i,\xi}}[k + \epsilon]s[p + k]e^{-\frac{2j\pi(k + \epsilon)\xi}{N}} \end{aligned} \quad (6)$$

For $t_i = p + \epsilon$, we have $\lfloor t_i \rfloor = p$ and $\{t_i\} = \epsilon$, which implies:

$$\mathcal{S}[i, \xi] = \sum_{k=-\infty}^{+\infty} \omega_{N,\theta_{i,\xi}}[k - \epsilon]s[p + k]e^{-\frac{2j\pi(k - \epsilon)\xi}{N}} \quad (7)$$

So the limit is the same for $t_i = p \pm \epsilon$ when $\epsilon \rightarrow 0$. \square

We have proved that our proposed STFT is continuous with respect to the frame index t_i . Let us now consider its differentiability with respect to t_i . Indeed, the integer and fractional part functions are differentiable everywhere except on integers. So Eq. (5) is differentiable everywhere except possibly when t_i takes an integer value. Using the fact that $\frac{\partial \lfloor t_i \rfloor}{\partial t_i} = 0$ and $\frac{\partial \{t_i\}}{\partial t_i} = 1$ for non integers t_i , we can easily show that:

$$\frac{\partial \mathcal{S}(i, \xi)}{\partial t_i} = \sum_{k=-\infty}^{+\infty} \tilde{\omega}_{N,\theta_{i,\xi}}[k - \{t_i\}]s[\lfloor t_i \rfloor + k]e^{-\frac{2j\pi(k - \{t_i\})\xi}{N}} \quad (8)$$

with $\tilde{\omega}_{N,\theta_{i,\xi}} = -\dot{\omega}_{N,\theta_{i,\xi}} + 2j\pi\xi\omega_{N,\theta_{i,\xi}}$ and $\dot{\omega}_{N,\theta_{i,\xi}}(u) = \frac{\partial \omega_{N,\theta_{i,\xi}}(u)}{\partial u}$. Extension to any value of t_i is the point of Prop. 3.2 below.

Proposition 3.2. *The modified STFT defined by Eq. (5) is everywhere differentiable w.r.t. t_i .*

Proof. Since the window $\omega_{N,\theta_{i,\xi}}$ is continuous function with continuous derivatives with respect to time variable, $\tilde{\omega}_{N,\theta_{i,\xi}}$ is still a continuous function with continuous derivatives with respect to time variable¹. Eq. (8) has then the same shape as Eq. (5) meaning a similar reasoning will show that the derivative Eq. (8) converges to the same limits when θ goes to an integer by lower or upper values. As a consequence, the proposed STFT is differentiable everywhere. \square

Remark 3.1. *Eq. 8 defines the derivatives with respect to the frame index t_i . As the hop length H_i is just the difference between consecutive frames indexes t_i and t_{i-1} , the derivatives with respect to hop length is straightforward.*

¹Both real and imaginary parts are continuous and differentiable with continuous derivatives with respect to time variable.

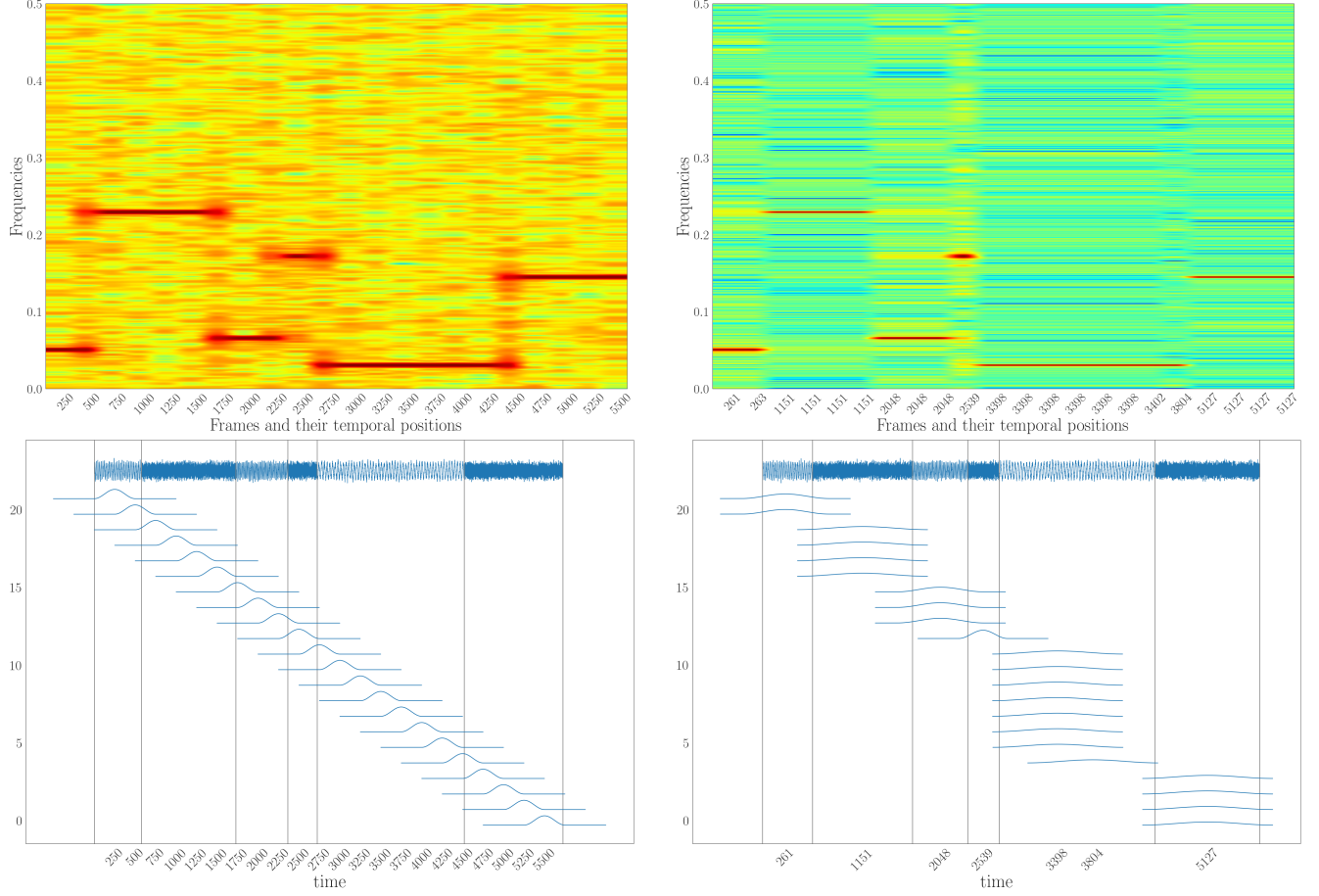


Figure 2: On the left side, we have the classical STFT and its frame temporal position along the signal. On the right side, we have the DSTFT with time-varying frame temporal position and window length, and the DSTFT frame temporal position along the signal.

Remark 3.2. Since the window length $\theta_{i,\xi}$ can vary within the support interval $[0, N]$, it would be more appropriate to define a "true" hop length $\tilde{H}_{i,\xi}$ that is computed as the difference between the positive starting points of two consecutive windows. This can be calculated using the following formula (see Fig. 1):

$$\begin{aligned}\tilde{H}_{1,\xi} &= H_1 + \frac{N - \theta_{1,\xi}}{2} \\ \tilde{H}_{i,\xi} &= H_i + \frac{\theta_{i,\xi} - \theta_{i-1,\xi}}{2} \quad \forall i > 1\end{aligned}\tag{9}$$

Then, the expression of derivatives with respect to $\tilde{H}_{i,\xi}$ is straightforward. One compelling reason to use the "true" hop length is that the window length may vary between frames in adaptive STFT with a time-varying window length.

Remark 3.3. In our differentiable STFT definition, we use one hop length parameter per frame. It is however possible to share parameters and suppose time invariance as in the classic STFT case to share only one window length and hop length.

4 Applications

In this section, we will show on a simulated signal that differentiable STFT with respect to both window length and hop length (or frame temporal position) can be of immediate interest and deserves more attention. We simulate a sinus of different frequencies with different temporal length. Classical STFT uses frames that are uniformly spread along the signal, which may not be the optimal positioning to localize frequency changes as frequencies have a variable length.

We initialize our differentiable STFT as classical STFT. In this application, we consider using time-varying window length. We then optimize the windows' temporal position and lengths by gradient descent according to a given criterion. More specifically, our goal is to find windows that are well-distributed over the overall signal, ensuring that there are no gaps and loss of information, and that allow for minimal energy leakage while achieving a better concentration of energy in the time-frequency plane. To promote energy concentration in each frame, we maximize the kurtosis of frame spectrum:

$$\mathcal{K}(\theta_i, \tilde{H}_i) = \frac{1}{\sum_{i=1}^T \omega_i} \sum_{i=1}^T \omega_i \frac{\mathbb{E}_\xi[\mathcal{S}[i, \xi]^4]}{\mathbb{E}_\xi[\mathcal{S}[i, \xi]^2]^2} \quad (10)$$

where ω_i is a weight used to minimize the contribution of windows that share the same segment of the signal. More specifically, we set $\omega_1 = t_2 - t_1$, $\omega_T = t_T - t_{T-1}$ and $\omega_i = \frac{t_{i+1} - t_{i-1}}{2}$ for every $i \in \{2, \dots, T-1\}$. To avoid information loss, we also want to maximize the spectrogram coverage²:

$$\mathcal{C}(\theta_i, \tilde{H}_i) = \frac{\sum_{i=1}^T \min(\theta_i, \tilde{H}_{i+1})}{M} \quad (11)$$

with $\tilde{H}_{T+1} = +\infty$ and M is the signal length. Finally, we use a multi-objective optimization to maximize both the energy concentration $\mathcal{K}(\theta_i, \tilde{H}_i)$ and the coverage of the spectrogram $\mathcal{C}(\theta_i, \tilde{H}_i)$ Désidéri [2012], Sener and Koltun [2018].³

We observe that the spectrogram obtained at the end of the optimization has a better concentration of energy due to reduced spectral leakage resulting from the proper positioning of frames, which are no longer straddling two different frequencies, as shown in Fig. 2. However, caution must be exercised when reading the time-axis of the resulting time-frequency representation as the distribution of frames is no longer uniform.

5 Conclusion

In conclusion, we have introduced a novel modification of the DSTFT, which makes this operation differentiable with respect to the hop length or frame temporal position. Through an example, we have demonstrated the benefit of using our differentiable STFT. Our proposed approach provides improved control over the temporal positioning of frames and enables the use of more computationally efficient optimization methods, such as gradient descent. Our differentiable STFT can also be easily integrated into existing algorithms and neural networks.

²Let's recall that in cases where the window's support extends beyond the signal, we zero-pad the signal for the calculation of the STFT. However, it's important to note that the coverage metric only takes into account the part of the window that overlaps with the signal.

³We have shared the notebook to reproduce the experiment at <https://github.com/maxime-leiber/dstft>.

References

- Kathleen M Stafford, Christopher G Fox, and David S Clark. Long-range acoustic detection and localization of blue whale calls in the northeast pacific ocean. *The Journal of the Acoustical Society of America*, 104(6):3616–3625, 1998.
- Jingshan Huang, Binqiang Chen, Bin Yao, and Wangpeng He. Ecg arrhythmia classification using stft-based spectrogram and convolutional neural network. *IEEE access*, 7:92871–92880, 2019.
- Q. Leclère, H. André, and J. Antoni. A multi-order probabilistic approach for instantaneous angular speed tracking debriefing of the cmmno14 diagnosis contest. *Mechanical Systems and Signal Processing*, 81:375–386, 2016.
- R. Stockwell, L. Mansinha, and R. Lowe. Localization of the complex spectrum: the S transform. *IEEE transactions on Signal Processing*, 44(4):998–1001, 1996.
- Ervin Sejdić, Igor Djurović, and Jin Jiang. A window width optimized s-transform. *EURASIP Journal on Advances in Signal Processing*, 2008:1–13, 2007.
- Ali Moukadem, Zied Bouguila, Djaffar Ould Abdeslam, and Alain Dieterlen. A new optimized stockwell transform applied on synthetic and real non-stationary signals. *Digital Signal Processing*, 46:226–238, 2015.
- R. N. Czerwinski and D. L. Jones. Adaptive short-time fourier analysis. In *IEEE Signal Processing Letters*, volume 4, pages 42–45, 1997.
- Henry K Kwok and Douglas L Jones. Improved instantaneous frequency estimation using an adaptive short-time fourier transform. *IEEE Transactions on Signal Processing*, 48:2964–2972, 2000.
- J. Zhong and Y. Huang. Time-frequency representation based on an adaptive short-time fourier transform. In *IEEE Transactions on Signal Processing*, volume 58, pages 5118–5128, 2010.
- S. Pei and S. Huang. STFT with adaptive window width based on the chirp rate. *IEEE Transactions on Signal Processing*, 60(8):4065–4080, 2012.
- Mingzhe Zhu, Xinliang Zhang, and Yue Qi. An adaptive stft using energy concentration optimization. In *International Conference on Information, Communications and Signal Processing (ICICSP)*, pages 1–4, 2015.
- A. Zhao, K. Subramani, and P. Smaragdis. Optimizing short-time fourier transform parameters via gradient descent. In *IEEE International Conference on Acoustics, Speech and Signal Processing (ICASSP)*, pages 736–740, 2021.
- Adam Jablonski and Kajetan Dziedziech. Intelligent spectrogram—a tool for analysis of complex non-stationary signals. *Mechanical Systems and Signal Processing*, 167:108554, 2022.
- S. Meignen, M. Colominas, and D. Pham. On the use of rényi entropy for optimal window size computation in the short-time fourier transform. In *IEEE International Conference on Acoustics, Speech and Signal Processing (ICASSP)*, pages 5830–5834, 2020.
- M. Leiber, A. Barrau, Y. Marnissi, and D. Abboud. A differentiable short-time fourier transform with respect to the window length. In *European Signal Processing Conference (EUSIPCO)*, pages 1392–1396, 2022a.
- Maxime Leiber, Axel Barrau, Yosra Marnissi, Dany Abboud, and Mohammed El Badaoui. Optimisation de la longueur de fenêtre du spectrogramme au sein d’un réseau de neurones. In *colloque GRETSI*, 2022b.
- M. Leiber, Y. Marnissi, A. Barrau, and M. El Badoui. Differentiable adaptive short-time fourier transform with respect to the window length. In *IEEE International Conference on Acoustics, Speech and Signal Processing (ICASSP)*, pages 1392–1396, 2023.
- Keunwoo Choi, György Fazekas, Mark Sandler, and Kyunghyun Cho. Convolutional recurrent neural networks for music classification. In *2017 IEEE International conference on acoustics, speech and signal processing (ICASSP)*, pages 2392–2396. IEEE, 2017.
- Giambattista Parascandolo, Heikki Huttunen, and Tuomas Virtanen. Recurrent neural networks for polyphonic sound event detection in real life recordings. In *2016 IEEE international conference on acoustics, speech and signal processing (ICASSP)*, pages 6440–6444, 2016.
- Miguel A Acevedo, Carlos J Corrada-Bravo, Héctor Corrada-Bravo, Luis J Villanueva-Rivera, and T Mitchell Aide. Automated classification of bird and amphibian calls using machine learning: A comparison of methods. *Ecological Informatics*, 4(4):206–214, 2009.
- Chih-Yuan Koh, Jaw-Yuan Chang, Chiang-Lin Tai, Da-Yo Huang, Han-Hsing Hsieh, and Yi-Wen Liu. Bird sound classification using convolutional neural networks. In *CLEF (Working Notes)*, 2019.
- Brian M Sadler, Tien Pham, and Laurel C Sadler. Optimal and wavelet-based shock wave detection and estimation. *The Journal of the Acoustical Society of America*, 104(2):955–963, 1998.

N. H. Chandra and A. Sekhar. Fault detection in rotor bearing systems using time frequency techniques. *Mechanical Systems and Signal Processing*, 72:105–133, 2016.

Jean-Antoine Désidéri. Multiple-gradient descent algorithm (mgda) for multiobjective optimization. *Comptes Rendus Mathématique*, 350(5-6):313–318, 2012.

Ozan Sener and Vladlen Koltun. Multi-task learning as multi-objective optimization. *Advances in neural information processing systems*, 31, 2018.